J. Fluid Mech. (1977), *vol.* 81, *part* 4, *pp.* 641–655
Printed in Great Britain

Hydrodynamic instability of viscous flow between rotating coaxial cylinders with fully developed axial flow

By K. C. CHUNG AND K. N. ASTILL

Department of Mechanical Engineering, Tufts University, Medford, Massachusetts 02155

(Received 23 August 1976)

A linear stability analysis is presented for flow between concentric cylinders when a fully developed axial flow is present. Small perturbations are assumed to be non-axisymmetric. This leads to an eigenvalue problem with four eigenvalues: the critical Taylor number, an amplification factor and two wavenumbers. The presence of the tangential wavenumber permits prediction of the stability of spiral flow. This made it possible to model the flow more accurately and to extend the range of calculations to higher axial Reynolds numbers than had previously been attainable. Calculations were carried out for radius ratios from 0·95 to 0·1, Reynolds numbers as large as 300 and cases with co-rotation and counter-rotation of the cylinders.

1. Introduction

Since G. I. Taylor (1923) predicted analytically the onset of instability in a Couette flow between coaxial rotating cylinders and demonstrated the validity of his results by a simple experiment, considerable research on the problem has been conducted both analytically and experimentally. When an axial flow is superimposed on the Couette flow, the problem becomes more complicated. This combined flow, so-called Couette–Poiseuille flow, occurs in numerous existing or proposed design applications.

Kaye & Elgar (1958) observed that four principal modes of flow exist: laminar, turbulent, laminar with vortices and turbulent with vortices. Numerous investigations have since been conducted to establish the effect of important variables on the occurrence of Taylor vortices in a laminar flow. The critical Taylor number Ta_c is determined as a function of the axial Reynolds number Re, the radius ratio N, the speed ratio of cylinder rotation μ and, in the case of developing flows, the inlet length L. In the 1960s and 1970s experimental studies were conducted with radius ratios of 0·89 $\sim$ 0·96 by Donnelly & Fultz (1960), Snyder (1962, 1965) and Coney & Mobbs (1970). Astill (1964) extended the work by Kaye & Elgar (1958) to developing flow. In the same period, several investigators studied the problem analytically, including Chandrasekhar (1960, 1962), DiPrima (1960), Krueger & DiPrima (1964), Datta (1965), Hughes & Reid (1968) and Elliot (1973).

The analytical studies to date have incorporated two main assumptions: (*a*) small gap, $R_2 - R_1 \ll \frac{1}{2}(R_1 + R_2)$, *and* (*b*) *linear perturbation theory with* axisymmetric perturbations. Solutions were limited to small Reynolds numbers with the exception of Hughes & Reid (1968). It is known from experiments that for Reynolds numbers above 15 $\sim$ 20 the vortices are no longer toroidal but form pairs of spirals.

The objective of the present study is to determine the critical Taylor numbers and the associated eigenvalues for fully developed flows in a concentric annulus of arbitrary radius ratio with one or both cylinders rotating. In order to represent the known physical behaviour and to extend the solution to higher Reynolds numbers, perturbations were assumed to be non-axisymmetric. While the present results are for fully developed axial flows, the formulation and solution method are equally applicable to developing flow, which is likely to be more important in applications. The fully developed solution is numerically simpler and provides a lower bound on the critical Taylor number for a given flow system.

2. Formulation of the problem

The Navier–Stokes and continuity equations are written in cylindrical co-ordinates for an incompressible fluid with constant viscosity in the absence of body forces. The equations are somewhat simplified by introducing a circulation function and then made non-dimensional by normalizing velocities with the mean axial velocity $\overline{W}$, lengths with the gap width b $(= R_2 - R_1)$, pressures with $\rho\overline{W}^2$ and time with $b/\overline{W}$. R_1 and R_2 are the radii of the inner and outer cylinders respectively and ρ is the fluid density. Linearization of the equations follows the usual procedure fully described by Chandrasekhar (1961), in which the velocities and pressure in the unstable flow are each expressed as the sum of their form in steady flow and a small perturbation. With ϕ' representing any of the perturbations, u' corresponding to the radial velocity, w' to the axial velocity and v' to a circulation function, a three-dimensional perturbation $\phi'(t, r, \theta, z)$ is assumed to have the form

$$\phi' = \hat{\phi}(r)\ \exp\{i(\sigma t + n\theta + \lambda z)\}, \tag{1}$$

where $\hat{\phi}$ is a complex amplitude function, and σ, n and λ are called the amplification factor, the tangential wavenumber and the axial wavenumber respectively. At the onset of oscillatory instability, σ should be real so that the time amplification is bounded. Also, for spatially bounded motion of the perturbation flow the wavenumbers n and λ must be real, and furthermore n must be an integer. Introducing the perturbations u', v', w' and p' into the linear equations and eliminating the amplitude function $\hat{p}$ of the perturbation pressure, the momentum equations become

$$d\hat{w}_2/dr = A_1\hat{u} + A_2\hat{v} + A_3\hat{v}_1 + A_4\hat{w} + A_5\hat{w}_1 + A_6\hat{w}_2, \tag{2}$$

$$d\hat{v}_1/dr = A_7\hat{u} + A_8\hat{v} + A_9\hat{v}_1 + A_{10}\hat{w} + A_{11}\hat{w}_1 + A_{12}\hat{w}_2. \tag{3}$$

The continuity equation is expressed in the form

$$d\hat{u}/dr = A_{13}\hat{u} + A_{14}\hat{v} + A_{15}\hat{w}. \tag{4}$$

The variable coefficients A_j $(j = 1, 2, \ldots, 12)$ are complex and contain the steady parts of the velocities, the Reynolds number, defined as $Re = \overline{W}b/\nu$, and the eigenvalues. The subscripts 1 and 2 on $\hat{u}$, $\hat{v}$ and $\hat{w}$ indicate the order of ordinary derivatives with respect to r of these amplitude functions. Accordingly, three additional relationships are

$$d\hat{v}/dr = \hat{v}_1, \quad d\hat{w}/dr = \hat{w}_1, \quad d\hat{w}_1/dr = \hat{w}_2. \tag{5}$$

Equations (2)–(5) constitute a set of first-order, linear, ordinary, homogeneous

differential equations with variable coefficients. Each variable and coefficient can be expressed in terms of a real and imaginary part:

$$\left.\begin{aligned} \hat{\phi} &= \bar{\phi} + i\tilde{\phi}, \quad \phi = u, v, w, \\ A_j &= \bar{A}_j + i\tilde{A}_j, \quad j = 1, 2, \ldots, 12. \end{aligned}\right\} \tag{6}$$

Substituting (6) into the equations and separating the real and imaginary parts leads to a set of twelve real differential equations in twelve unknowns. The Taylor number, defined as $Ta = \Omega_1 R_1 b/\nu$, is in most instances hidden in the coefficients $\bar{A}_j$ and $\tilde{A}_j$. In order to include the Taylor number explicitly, partial renormalization of the steady part of the dimensional circulation function with $\Omega_1 R_1$ instead of $\overline{W}$ is necessary, where Ω_1 is the angular speed of the inner cylinder. For a complete development of the equations see Chung (1976).

To complete the statement of the problem, twelve boundary conditions for the perturbation velocities are required. The no-slip condition holds at the walls:

$$\bar{u} = \tilde{u} = \bar{v} = \tilde{v} = \bar{w} = \tilde{w} = 0 \quad \text{at} \quad r = r_1, r_2. \tag{7), (8}$$

A shooting procedure was employed in which the problem is treated as an initial-value problem at $r = r_1$. Six additional boundary conditions are assumed at r_1 and the solution repeatedly marched to r_2 until the terminal boundary conditions (8) are satisfied with trial eigenvalues. The difficult task of guessing the correct missing boundary conditions at r_1 can be avoided if each perturbation velocity is expressed as a linear combination of component velocities with undetermined coefficients C_j ($j = 1, 2, \ldots, 6$) (Sparrow, Munro & Jonsson 1964):

$$\left.\begin{aligned} \bar{w}_i &= \sum_{j=1}^{6} C_j \bar{w}_i^j, \quad \tilde{w}_i = \sum_{j=1}^{6} C_j \tilde{w}_i^j, \quad i = 0, 1, 2, \\ \bar{v}_i &= \sum_{j=1}^{6} C_j \bar{v}_i^j, \quad \tilde{v}_i = \sum_{j=1}^{6} C_j \tilde{v}_i^j, \quad i = 0, 1, \\ \bar{u}_i &= \sum_{j=1}^{6} C_j \bar{u}_i^j, \quad \tilde{u}_i = \sum_{j=1}^{6} C_j \tilde{u}_i^j, \quad i = 0. \end{aligned}\right\} \tag{9}$$

Shooting is carried out first for $j = 1$, with initial boundary conditions $\bar{v}_1 = 1$ and $\tilde{v}_1 = \bar{w}_1 = \tilde{w}_1 = \tilde{w}_2 = \bar{w}_2 = 0$ in addition to the initial conditions (7) at r_1, then for $j = 2$ with $\tilde{v}_1 = 1$ and $\bar{v}_1 = \bar{w}_1 = \tilde{w}_1 = \bar{w}_2 = \tilde{w}_2 = 0$ with (7). Similarly, shooting continues for $j = 3$ with $\bar{w}_1 = 1$ and the other velocities zero and so on. Summation of the six component velocities after completion of the shooting leads to a set of solutions for the unknowns which could be solved identically with additional boundary conditions $\bar{v}_1 = C_1$, $\tilde{v}_1 = C_2$, $\bar{w}_1 = C_3$, $\tilde{w}_1 = C_4$, $\bar{w}_2 = C_5$ and $\tilde{w}_2 = C_6$ at r_1 if $C_1, C_2, \ldots, C_6$ were known.

Since the differential equations are linear and homogeneous, the solution modes for each shooting are independent of the magnitude of the C_j. Therefore the terminal boundary conditions (8) lead to six linear algebraic homogeneous equations, which in matrix form are

$$\begin{pmatrix} \bar{u}^1 & \bar{u}^2 & \bar{u}^3 & \bar{u}^4 & \bar{u}^5 & \bar{u}^6 \\ \tilde{u}^1 & \tilde{u}^2 & \tilde{u}^3 & \tilde{u}^4 & \tilde{u}^5 & \tilde{u}^6 \\ \bar{v}^1 & \bar{v}^2 & \bar{v}^3 & \bar{v}^4 & \bar{v}^5 & \bar{v}^6 \\ \tilde{v}^1 & \tilde{v}^2 & \tilde{v}^3 & \tilde{v}^4 & \tilde{v}^5 & \tilde{v}^6 \\ \bar{w}^1 & \bar{w}^2 & \bar{w}^3 & \bar{w}^4 & \bar{w}^5 & \bar{w}^6 \\ \tilde{w}^1 & \tilde{w}^2 & \tilde{w}^3 & \tilde{w}^4 & \tilde{w}^5 & \tilde{w}^6 \end{pmatrix} \begin{pmatrix} C_1 \\ C_2 \\ C_3 \\ C_4 \\ C_5 \\ C_6 \end{pmatrix} = 0 \quad \text{at} \quad r = r_2. \tag{10}$$

A non-trivial solution for the C_j requires the determinant of the 6×6 matrix to vanish. Notice that the characteristic equation in (10) is independent of the coefficients.

Solutions for a particular geometry and Reynolds number are obtained by first introducing a trial set of eigenvalues Ta, σ, n and λ. Using a fourth-order Runge–Kutta scheme, shooting is performed six times, once for each component group. The determinant can then be evaluated. If the determinant vanishes, a set of modes has been found with a group of probable eigenvalues. The critical Taylor number is identified as the smallest Taylor number found among all groups of probable eigenvalues.

3. Numerical procedure

The requirement that the determinant should vanish is expressed in a functional form:

$$\det = F(Ta, \sigma, n, \lambda) = 0. \tag{11}$$

Since (11) yields $Ta = f(\sigma, n, \lambda)$, minimizing Ta requires

$$\frac{\partial Ta}{\partial \sigma} = \frac{\partial Ta}{\partial n} = \frac{\partial Ta}{\partial \lambda} = 0. \tag{12}$$

In reality it is not possible to cause the determinant to be identically zero. Therefore the determinant is instead minimized with respect to the eigenvalues:

$$\frac{\partial F}{\partial Ta} = \frac{\partial F}{\partial \sigma} = \frac{\partial F}{\partial n} = \frac{\partial F}{\partial \lambda} = 0. \tag{13}$$

Conditions (13) and (12) were used as basic criteria for the critical Taylor number and associated eigenvalues.

In the iteration procedure to determine the critical values it is known (i) that the critical Taylor number increases monotonically with axial Reynolds number and (ii) that the tangential wavenumber should be an integer and increase with Reynolds number. Starting with available values of Ta_c and λ found by Sparrow *et al.* (1964) and Astill & Chung (1976) with $\sigma = n = 0$ for $Re = 0$, iteration continues for increasing Re. For a guessed Ta and n, the minimum determinant is obtained by iteration of a pair (β, λ), where β is defined as the ratio $-\sigma/\lambda$. The results of this search are shown graphically in figure 1. β was found to be more sensitive than λ in the determination of the minimum determinant and remained almost unchanged in the neighbourhood of the given Ta when n remained the same. Therefore, in searching for β and λ, the increment $\Delta\beta$ was kept as small as possible. Once β had been found for a given Ta only a little more iteration of β was necessary for the adjacent values of Ta. Loci of the minimum determinant in figure 1 are shown in figure 2 as solid and dashed curves for a wide range of Ta. The dashed curves result from improper selection of n for the range of Ta. In the figure Ta_1 is the most likely value of the critical Taylor number with $n = n_1$. When the minimum determinant in the region of $n = n_2$ is only slightly larger than that near n_1, it is safer to select both Ta_1 and Ta_2 as critical values. Usually in this case Ta_1 and Ta_2 are very close. One Fortran program handles the procedure of selecting n and β as well as approximating λ and Ta_c as shown in figures 1 and 2. Another program iterates Ta_c and λ with the appropriate values of n and β.

Arithmetic precision appeared to be important in terms of the range of Re. Single-precision computation worked well only when the Reynolds number was low, say

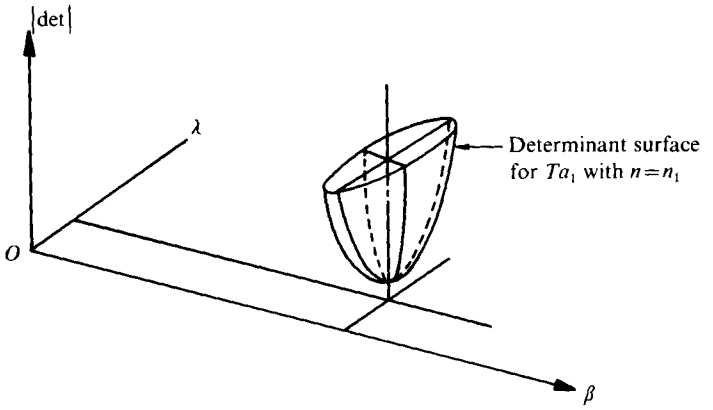

FIGURE 1. Schematic representation of searching for a combination (β, λ) which gives the minimum determinant for a given Ta and n.

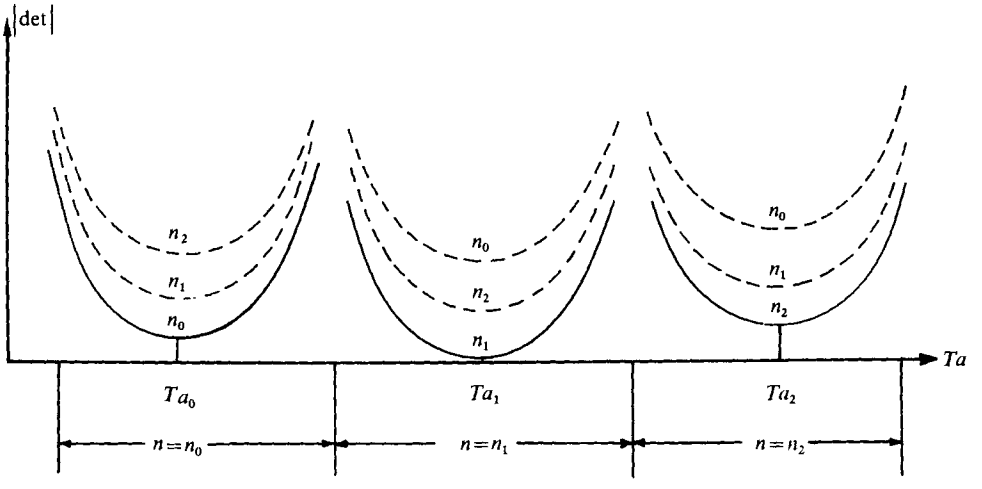

FIGURE 2. Schematic representation of searching for the critical Taylor number with variation of the tangential wavenumber n.

$Re < 100$, for $N = 0{\cdot}95$. For higher values of Re numerical error caused the determinant data to be scattered, owing to which determination of critical values was not decisive. Double-precision arithmetic extended the computable range of Re considerably, giving clear differentiation among the critical values.

The step size of the Runge–Kutta integration also influenced the values of Ta_c. Theoretically more steps will give greater accuracy. On the basis of trial calculations employing 10, 20 and 30 steps, a 20-step calculation was used throughout the iteration.

4. Results and discussion

The present analysis was performed for the case where the instability occurs in fully developed flow. The steady parts of the axial velocity and circulation function are respectively

$$W_{fd} = 2\frac{1+(r/r_2)^2+[(N^2-1)/\ln N]\ln(r/r_2)}{1+N^2-(N^2-1)/\ln N} \tag{14}$$

Re	n	λ	β	Ta_c
0	0	3·128	0	184·991
0·1	0	3·133	1·171	184·992
1	0	3·154	1·171	185·072
2	0	3·157	1·171	185·29
5	0	3·172	1·171	186·79
10	0	3·17	1·17	192·06
20	1	3·07	1·26	211·8
35	2	3·04	1·29	261·0
50	4	3·47	1·37	323·2
75	7	3·05	1·55	444·6
100	10	2·81	1·76	553
	11	2·90	1·80	547
150	12	2·76	1·84	752
	13	2·26	2·09	751
	14	2·31	2·13	739
200	14	2·27	2·08	920
	15	2·03	2·28	915
	16	2·02	2·36	907
300	16	1·78	2·39	1218
	17	1·75	2·48	1200

TABLE 1. Critical Taylor numbers and corresponding values of n, λ and β for given values of Re when $N = 0{\cdot}95$ and $\mu = 0$.

and
$$V_{fd}^* = -\frac{N^2(1-\mu/N^2)}{r_1(1-N^2)}r^2 + \frac{1-\mu}{1-N^2}r_1, \tag{15}$$

where $\mu = \Omega_2/\Omega_1$ and $N = R_1/R_2$. The fully developed circulation function V_{fd}^* has been made non-dimensional with $\Omega_1 R_1$. Since the governing equations are general, solution is possible for any cylinder geometry as long as $\mu/N^2 < 1$ (Rayleigh's criterion for instability). Computations were performed for $N = 0{\cdot}95$, $0{\cdot}75$, $0{\cdot}5$, $0{\cdot}25$ and $0{\cdot}1$ with the inner cylinder rotating. Calculations were made for Reynolds numbers as large as $300 \sim 400$. Solutions with both cylinders rotating were obtained for $N = 0{\cdot}95$ with $Re \leqslant 200$. Referring to the solutions by Sparrow *et al.* (1964) and by Astill & Chung (1976), solutions were evaluated and compared for $Re = 0$ in the geometries and conditions of the earlier work.

Inner cylinder rotating

In table 1 the variation of the critical Taylor number Ta_c with Reynolds number for $N = 0{\cdot}95$ and $\mu = 0$ is tabulated with the associated eigenvalues β, n and λ. Since in the first few cases the Reynolds number increases in small steps, three significant figures past the decimal point were retained to differentiate among the results. β remains almost unchanged for low values of Re. The axial wavenumber λ increases slightly with Re. For $Re = 20$ the presence of a single pair of vortex spirals was evident. Both the determinant and Ta_c with $n = 0$ were a little larger than those with $n = 1$, which suggests that for $Re = 20$ the prevailing secondary flow is spiral. For higher Reynolds numbers, each case requires several trial values of n. Two or three n's are listed with the other eigenvalues as possible values for the critical state. Here determination was not decisive since the determinant increases only a little with n while Ta_c decreases. Whenever the number of spirals increased, the magnitude of λ and β also changed

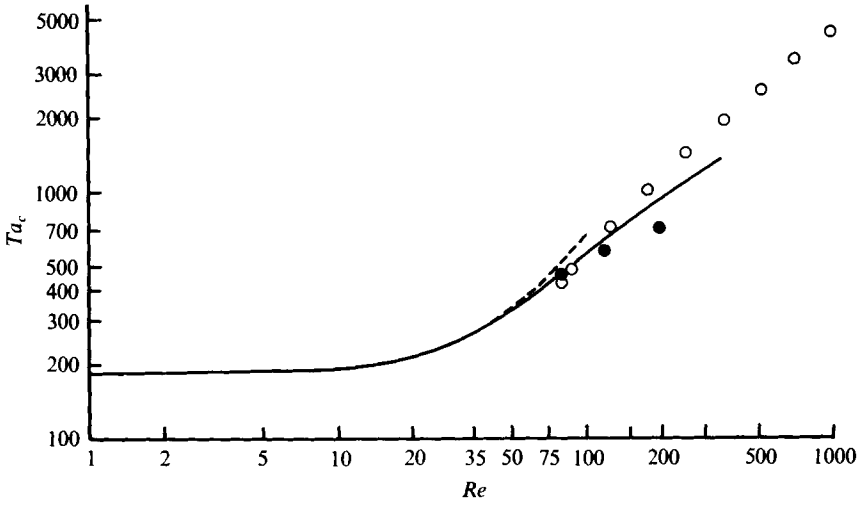

FIGURE 3. Comparison of the critical Taylor numbers Ta_c when $N = 0{\cdot}95$ and $\mu = 0$. ○, Hughes & Reid (1968), $N \to 1$; ●, Snyder (1965), $N = 0{\cdot}96$; ——, present non-axisymmetric results; – – –, present axisymmetric results.

drastically, which was first observed numerically in the present analysis. It should be noticed that the sudden increase in β is not because of a large change in σ, but rather because of a step decrease in the axial wavenumber λ. The decrease in λ implies that with the increasing number of spirals the axial wavelength also increases drastically, adjusting to the new pattern of spiral flow. Beyond $Re = 300$ determination of Ta_c etc. was not conclusive.

In figure 3 the results of Hughes & Reid (1968) and the experimental results of Snyder (1965) are compared with the present non-axisymmetric results. The results of Hughes & Reid (1968) were based on a small gap and axisymmetric perturbations for the high Reyholds number domain, where the dominant mechanism of instability is of the Tollmien–Schlichting type. For interest, solutions were obtained under the assumption of axisymmetry ($n = 0$) and are compared with various results found by others and with the present non-axisymmetric results in table 2 and figure 4. The conventional Taylor number Ta_c^* is used for direct comparison. The relationship between the two Taylor numbers is $Ta^* = 2\,Ta^2 b/(R_1 + R_2)$. The overall results for Ta_c^* agree closely up to $Re = 50$ but differ by as much as a factor of two for $Re = 100$ on the Ta_c^* scale. The results of Krueger & DiPrima (1964), which are an improvement on DiPrima's previous work (1960), are very close to the present results in the range of Re computed. The recent data obtained by Elliot (1973) were based on the same approach as that of Krueger & DiPrima (1964), but were obtained with more terms in the trial eigenfunctions in the Galerkin formulation. Elliot's results agree best with the present axisymmetric results in the entire range of Re considered. The analyses by Sparrow *et al.* (1964) and by Astill & Chung (1976) indicate that, for $Re = 0$, Ta_c^* decreases with increasing radius ratio in the vicinity of $N = 0{\cdot}95$. Consequently, it is expected that the values of Ta_c^* for the small-gap approximation ($N \simeq 1$) should be lower than those for $N = 0{\cdot}95$ from the present axisymmetric solution at least for low Reynolds numbers. The values of λ and β for the axisymmetric

	(a)			(b)			(c)			(d)		
Re	λ	β	Ta_c^*	λ	β	Ta_c^*	λ	β	Ta_c^*	λ	$W_d/\overline{W}$	Ta_c^*
0	3·1	—	1715	3·12	—	1696	—	—	—	3·23	—	1710
1	—	—	—	3·13	1·17	1698	3·12	1·17	1696	—	—	—
2 (0·02)†	—	—	—	—	—	—	3·12	1·17	1700	3·15	1·19	1823
5 (0·17)‡	3·1	0·813	1753	3·13	1·17	1729	3·13	1·17	1729	3·11	1·19	1883
10 (0·34)‡	—	—	—	3·13	1·16	1838	3·14	1·17	1832	—	—	—
20 (0·67)‡	3·4	0·819	2309	3·17	1·16	2236	3·16	1·165	2275	—	1·16	2400
40	4·2	0·839	3881	3·20	1·15	4025	3·21	1·155	4036	3·40	1·16	4088
60	5·2	0·866	5962	3·13	1·14	7459	3·2	1·14	7430	3·96	—	6850
80	6·0	0·885	8319	—	—	—	2·97	1·12	12810	4·75	1·07	9550
100	6·6	0·900	10876	—	—	—	2·61	1·08	20340	5·40	—	12700

	(e)				(f)			
Re	*n*	λ	β	Ta_c^*	*n*	λ	β	Ta_c^*
0	0	3·128	—	1755	0	3·128	—	1755
1	0	3·154	1·171	1756	0	3·154	1·171	1756
5	0	3·172	1·171	1789	0	3·154	1·171	1789
10	0	3·17	1·17	1892	0	3·17	1·17	1892
20	1	3·07	1·26	2300	0	3·36	1·17	2322
35	2	3·04	1·29	3493	0	3·46	1·16	3563
50	4	3·47	1·37	5356	0	3·50	1·16	5649
75	7	3·05	1·55	10137	0	3·65	1·15	11571
100	11	2·90	1·80	15344	0	3·68	1·15	21600

† Results (*d*). ‡ Results (*c*).

TABLE 2. Comparison of the present results with existing data for the case $N = 0{\cdot}95$ and $\mu = 0$. (*a*) Variational method of Chandrasekhar (1960). (*b*) Galerkin method of Krueger & DiPrima (1964). (*c*) Galerkin method of Elliot (1973). (*d*) Experiment of Snyder (1962). (*e*) Non-axisymmetric and (*f*) axisymmetric solution from the present analysis. (*a*)–(*c*) $N \to 1$ with approximate profiles of axial and tangential velocity. (*d*) $N = 0{\cdot}948$.

case from the present and other analyses are in close agreement. λ increases monotonically with *Re* while β decreases slightly. The ratio β can be identified as the ratio of the drift velocity of the vortices to the mean axial velocity: $W_d/\overline{W}$. This has been measured experimentally. In the non-axisymmetric solution the variation of λ and β with *Re* was different. λ appeared to increase slightly with *Re* while *n* remained constant, but whenever *n* increased a sudden drop occurred in λ, which in turn resulted in a step increase in β. The difference in the variation of λ and β between the present results and Snyder's experiments (1962, 1965) remains unexplained.

The variation of Ta_c with *Re* is given in tables 3 and 4 for $N = 0{\cdot}75$ and $0{\cdot}5$ with $\mu = 0$. The results for λ and β behave similarly to those for $N = 0{\cdot}95$. The tangential wavenumbers *n* are smaller than those for $N = 0{\cdot}95$, which implies that there are fewer spirals in the flow in a larger gap. Results for $N = 0{\cdot}25$ and $0{\cdot}1$, which are not listed here in detail, show that the secondary flows for these two cases are always axisymmetric ($n = 0$) in the range of Reynolds numbers investigated: $Re \leqslant 150$ for $N = 0{\cdot}25$ and $Re \leqslant 100$ for $N = 0{\cdot}1$. For these small radius ratios, iteration was easier because *n* is a small integer and an improper selection of *n* would cause a distinctive change in the determinant and consequently in Ta_c.

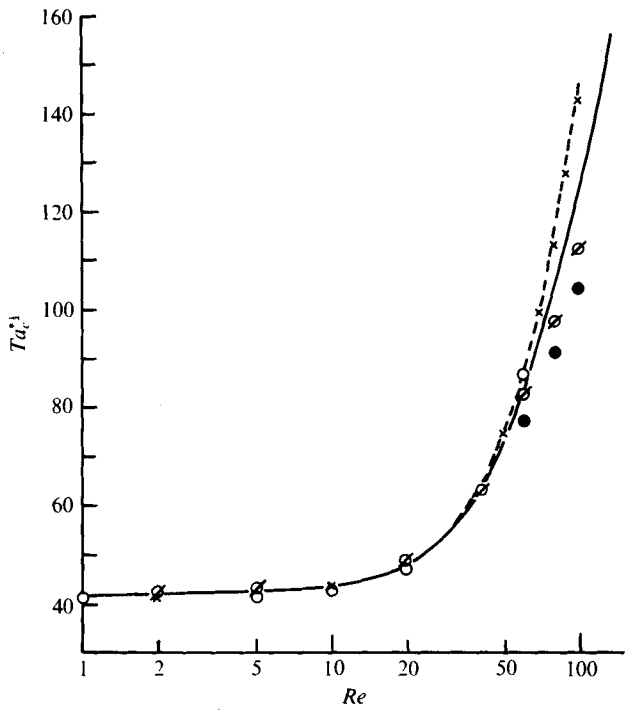

FIGURE 4. Comparison of the critical Taylor numbers Ta_c^* with existing data. ——, present non-axisymmetric results; – – –, present axisymmetric results; ●, Chandrasekhar (1960); ⌀, experiment by Snyder (1962); ○, Krueger & DiPrima (1964); ×, Elliot (1973). All point data are for $N \to 1$ except Snyder's, for which $N = 0{\cdot}948$.

Re	n	λ	β	Ta_c
0	0	3·135	0	85·779
0·1	0	3·146	1·172	85·780
1	0	3·144	1·172	85·812
2	0	3·148	1·172	85·991
5	0	3·163	1·172	86·60
10	0	3·165	1·171	89·02
20	1	3·14	1·40	98·1
35	1	2·82	1·34	120·5
50	1	2·95	1·30	148·8
75	2	2·32	1·52	204·6
100	2	2·20	1·52	258
150	3	1·62	1·86	319
200	3	1·30	1·95	375
300	3	1·03	2·00	465

TABLE 3. Critical Taylor numbers and corresponding values of n, λ and β for given values of Re when $N = 0{\cdot}75$ and $\mu = 0$.

Re	n	λ	β	Ta_c
0	0	3·151	0	68·189
0·1	0	3·154	1·181	68·189
1	0	3·175	1·181	68·214
2	0	3·178	1·181	68·290
5	0	3·192	1·181	68·818
10	0	3·190	1·180	70·67
20	0	3·074	1·174	77·90
35	0	3·04	1·164	96·0
50	0	2·96	1·15	120·8
	1	2·51	1·48	114·2
75	1	2·87	1·39	146·1
100	1	2·52	1·40	184
150	1	2·10	1·42	251
200	1	1·61	1·49	299
300	1	1·25	1·52	369

TABLE 4. Critical Taylor numbers and corresponding values of n, λ and β for given values of Re when $N = 0{\cdot}5$ and $\mu = 0$.

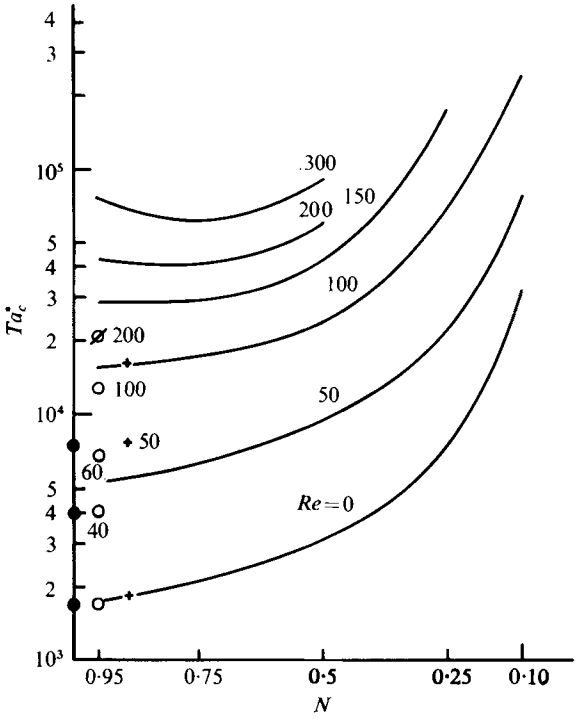

FIGURE 5. Variation of the critical Taylor number Ta_c^* with the radius ratio N and the Reynolds number Re. ——, present results; ○, Snyder (1962); ⌀, Snyder (1965); ●, Krueger & DiPrima (1964); +, Coney & Mobbs (1970).

Re	Present analysis				Krueger & DiPrima (1964)		
	n	λ	β	Ta_c^*	λ	β	Ta_c^*
		$\mu = 0{\cdot}45$			$\mu = 0{\cdot}5$		
0	0	3·14	0	2378	3·11	0	2278
1	0	3·12	1·17	2380	3·11	1·17	2280
5	0	3·14	1·17	2424	3·11	1·17	2322
10	—	—	—	—	3·13	1·17	2456
20	1	3·02	1·32	3141	3·15	1·17	3006
40	—	—	—	—	3·17	1·15	5420
50	3	3·01	1·44	7645	—	—	—
100	5	2·11	1·80	28693	—	—	—
	6	1·93	2·04	29465	—	—	—
200	8	1·34	2·80	94991	—	—	—
	9	1·30	3·05	92082	—	—	—
		$\mu = -1{\cdot}0$			$\mu = -1{\cdot}0$		
0	0	4·21	0	5310	4·0	0	4724
1	0	4·19	1·10	5314	4·0	1·14	4725
5	0	4·17	1·10	5371	4·0	1·11	4773
10	—	—	—	—	4·0	1·10	4915
20	1	3·43	1·20	6257	4·1	1·10	5436
40	—	—	—	—	4·2	1·07	6967
50	4	2·92	1·30	8287	—	—	—
100	8	2·32	1·40	16313	—	—	—
200	10	2·10	1·48	36530	—	—	—

TABLE 5. Comparison of the present results for both cylinders rotating and $N = 0{\cdot}95$ with those of Krueger & DiPrima (1964) for $N \to 1$.

The overall results for Ta_c^* are shown in figure 5 cross-plotted with various radius ratios for several Reynolds numbers. Included on the curves for comparison are some representative experimental and analytical results from other researchers.

Both cylinders rotating

The cases with both cylinders rotating were computed in the same manner for $N = 0{\cdot}95$ with $Re = 0 \sim 200$. A single case was considered for each type of rotation: $\mu = 0{\cdot}45$ for co-rotation and $\mu = -1$ for counter-rotation. For the counter-rotating case the determinant data showed some scatter, which was also encountered by Sparrow *et al.* (1964) and by Astill & Chung (1976) at $Re = 0$. The behaviour of β, n and λ was similar to that with $\mu = 0$. The number of spirals for these two cases was a little smaller than that with only the inner cylinder rotating at the same Reynolds number. As shown in table 5 and in figure 6, the trend of the results for Ta_c^* agree well with those found by Krueger & DiPrima (1964) and by Snyder (1965) for both cases. Since the results of Snyder shown in figure 5 were plotted from the figures of his paper (1965), they can give only an approximate comparison. The difference in Ta_c^* between the results of Krueger & DiPrima (1964) and Snyder (1965) seems to be partly due to the difference in the radius ratios: Snyder's apparatus had a finite gap ($N = 0{\cdot}959$) while the analysis of Krueger & DiPrima was based on a small gap ($N \simeq 1$). Beyond $Re = 80$ the overall results for Ta_c^* of Snyder are lower than the present results and the difference increases with Re.

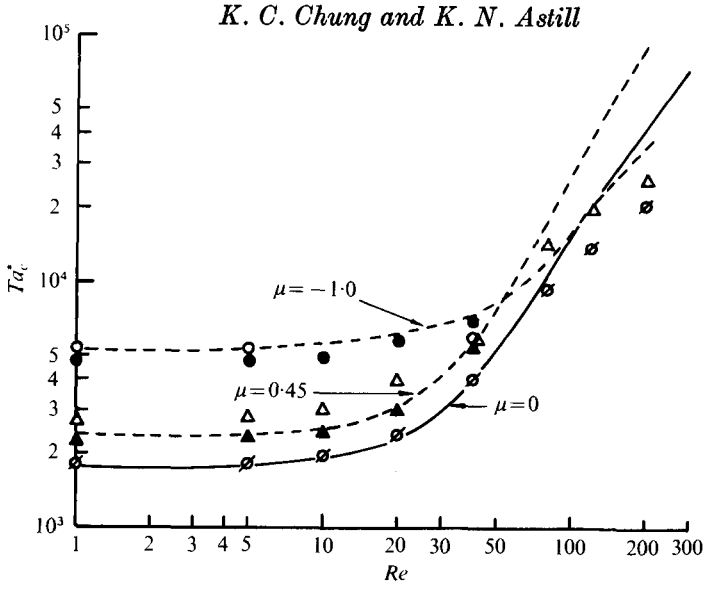

FIGURE 6. Comparison of the variations of the critical Taylor number Ta_c^* with μ and Re for $N = 0{\cdot}95$. The curves represent the present results. Snyder (1965), $N = 0{\cdot}96$: ∅, $\mu = 0$; △, $\mu = 0{\cdot}5$; ○, $\mu = -1{\cdot}0$. Krueger & DiPrima (1964), $N \to 1$: ▲, $\mu = 0{\cdot}5$; ●, $\mu = -1{\cdot}0$.

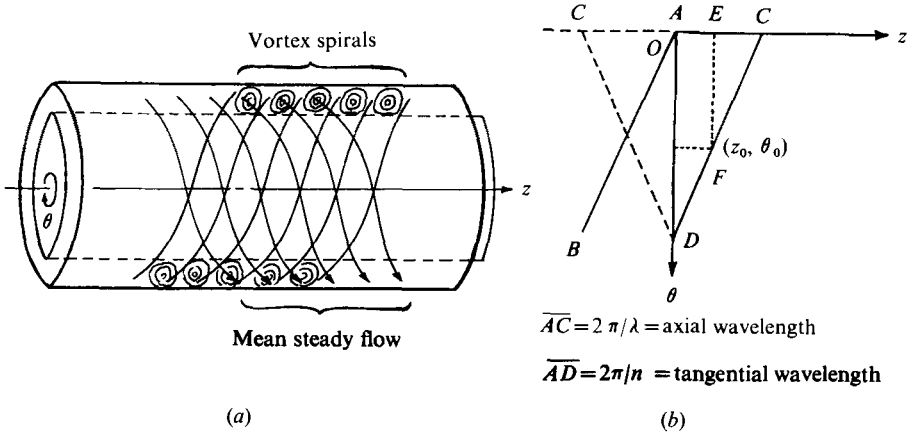

FIGURE 7. (*a*) Schematic representation of the direction of the mean steady flow and the inclination of the vortex spirals. (*b*) Drawing for inspection of spiral inclination.

Direction of spiral inclination

It is possible, from the present analysis, to determine the inclination of the vortex spirals with respect to the direction of the steady flow velocity. Consider the argument $\sigma t + n\theta + \lambda z$ in the perturbation (1). Let the time be fixed as zero. Then set the spatial co-ordinates of point A at the origin (0, 0) in figure 7 (*b*), where $\overline{AC}$ and $\overline{AD}$ are defined. A perturbation mode at A, say mode A, will reappear at C, D and C'. What happens at F, an arbitrary point on CD? Between A and F the increment of the argument is

$$n\theta_0 + \lambda z_0 = n(\overline{AD}/\overline{AC})\,\overline{CE} + \lambda(\overline{AC} - \overline{CE})$$
$$= n\left(\frac{2\pi}{n}\right)\left(\frac{\lambda}{2\pi}\right)\overline{CE} + \lambda\left(\frac{2\pi}{\lambda} - \overline{CE}\right) = 2\pi.$$

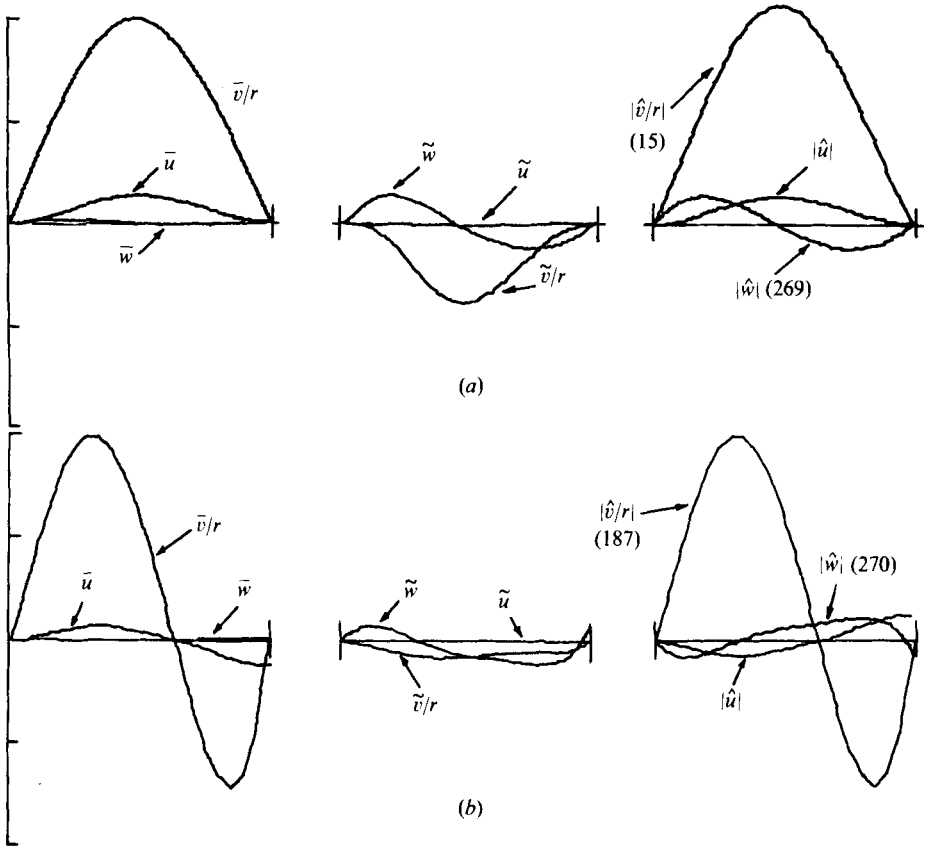

FIGURE 8. Mode shapes: real and imaginary parts of the amplitude functions and maximum real parts of the perturbation modes. Figures in brackets are phase-angle differences (degree) of the perturbation velocities from the radial perturbation velocities. $N = 0{\cdot}95$, $n = 0$. (*a*) $Re = 10$, $\mu = 0, \lambda = 3{\cdot}170, \beta = 1{\cdot}170, Ta = 192{\cdot}06$. (*b*) $Re = 1, \mu = -1, \lambda = 4{\cdot}190, \beta = 1{\cdot}098, Ta = 321{\cdot}866$.

A similar inspection at an arbitrary point on $C'D$ does not produce 2π, which implies that mode A can appear only along CD and on lines parallel to CD equally spaced in the z direction by an axial wavelength $2\pi/\lambda$. Therefore, from simple inspection of the argument, it is concluded that inclination of the vortex spirals is in the direction opposite to that of the mean flow as shown in figure 7 (*a*), which agrees with Snyder's (1965) observation.

Mode shapes of the perturbation velocities

When mode shapes are to be computed at the critical state, the undetermined coefficients C_j ($j = 1, 2, \ldots, 6$) must be found. Since the system of algebraic equations (12) is homogeneous, the determinant should vanish for a non-trivial solution for the C_j, which is generally not possible. Therefore an approximate method was employed. Equations (12) are expressed as

$$[B_{ij}]_{\text{crit}}\{C_j\} = \{S_i\}, \quad i,j = 1, 2, \ldots, 6, \tag{16}$$

where S_i represents a residual. Minimizing the sum of the residuals ΣS_i^2 leads to an approximate solution for the C_j ($j = 2, 3, \ldots, 6$) with $C_1 = 1$. An example of the perturbation modes is shown in figure 8 (*a*). v'/r represents the tangential component of the

perturbation velocity. The real part of the perturbation velocity, which can be realized physically, is

$$\mathscr{R}\{\phi'(r,\theta,z,t)\} = \bar{\phi}\cos\alpha - \hat{\phi}\sin\alpha, \tag{17}$$

where $\alpha = \sigma t + n\theta + \lambda z$ is constant at a given time and at a given point. The maximum mode shape and its phase angle α can be numerically computed in the range $0 \leqslant \alpha \leqslant 2\pi$. The maximum mode shape can be obtained directly by taking its magnitude

$$|\phi'| = (\bar{\phi}^2 + \hat{\phi}^2)^{\frac{1}{2}}$$

if the phase angle is not required. Equation (17) can be expressed as

$$\mathscr{R}\{\phi'(r,\theta,z,t)\} = |\hat{\phi}|\cos\{\alpha + K_{\phi'}(r)\}, \tag{18}$$

where $K_{\phi'}$ is a variable phase angle which would be constant for $Re = 0$. The phase difference between u' and v'/r is known to be $2m\pi$ ($m = 0$ or 1) and that between u' and w' to be $\frac{1}{2}\pi + m\pi$ ($m = 0$ or 1) for $Re = 0$. Figure 8 (*a*) implies that in the presence of axial flow the phase differences among the maximum perturbation modes vary with the Reynolds number.

For counter-rotating cases the mode shapes hardly satisfy the terminal boundary conditions (8) as shown in figure 8 (*b*). This was expected from the fact that for $\mu < 0$ the determinant data had been somewhat scattered.

5. Conclusion

The method of solution described in this paper is simple in formulation but numerically as complicated as an experiment. The non-axisymmetric perturbations allow the solution to be extended to high Reynolds number for any gap width or type of cylinder rotation. The present results for the critical Taylor number for the axisymmetric case agree very closely with the recent analytical data of others. The non-axisymmetric results generally agree well with limited experimental data, except for the variation of the axial wavenumber λ with the Reynolds number Re. In the present analysis the axial wavelength appeared to increase with Reynolds number whenever the number of spirals increased. It was also confirmed that the inclination of the vortex spirals is opposite in direction to the mainstream.

After this paper was submitted for publication, two recently completed analyses of the flow stability in this geometry have come to the attention of the authors. Both treated the case of fully developed axial flow and should be mentioned. Hasoon & Martin (1977) predicted a critical Taylor number and critical wavenumbers for axisymmetric flow. Using both a time-dependent finite-difference procedure and a solution employing the Galerkin method, they computed results for radius ratios between 0·81 and 0·95 and for Reynolds numbers up to 1000. Thomas (1974) treated the non-axisymmetric or spiral case, employing the same formulation as is used in the present paper. His solution differed from the present case in the shooting procedure used to solve the complex differential equations. Thomas used three shootings rather than the six shootings required in the analysis reported here. Thomas (1974) computed results for a radius ratio of 0·895 and for Reynolds numbers less than 63.

Because of the radius ratios chosen by the several authors, it is difficult to compare results. It is fair to say that there is good agreement among the critical Taylor numbers

predicted. Differences are apparent among the critical axial wavenumbers predicted by the three studies. A detailed comparison of the three analyses should perhaps be undertaken in the near future.

The present method can be directly extended to problems (i) with a developing main flow and (ii) with a temperature gradient between the two vertical cylinders either with or without the steady axial flow.

The numerical work was done with PDP-10 time-sharing system in the Computer Center of Tufts University. Fruitful comments made by Professor L. M. Trefethen are gratefully acknowledged.

REFERENCES

ASTILL, K. N. 1964 *J. Heat Transfer, Trans. A.S.M.E.* C **86**, 383.
ASTILL, K. N. & CHUNG, K. C. 1976 *A.S.M.E. Paper* no. 76-FE-27.
CHANDRASEKHAR, S. 1960 *Proc. Nat. Acad. Sci.* **46**, 141.
CHANDRASEKHAR, S. 1961 *Hydrodynamic and Hydromagnetic Stability*. Oxford: Clarendon Press.
CHANDRASEKHAR, S. 1962 *Proc. Roy. Soc.* A **265**, 188.
CHUNG, K. C. 1976 Ph.D. thesis, Tufts University, Massachusetts.
CONEY, J. E. R. & MOBBS, F. R. 1970 *Proc. Inst. Mech. Engng* **184** (3L), 10.
DATTA, S. L. 1965 *J. Fluid Mech.* **21**, 635.
DIPRIMA, R. C. 1960 *J. Fluid Mech.* **9**, 621.
DONNELLY, R. J. & FULTZ, D. 1960 *Proc. Nat. Acad. Sci.* **46**, 1150.
ELLIOT, L. 1973 *Phys. Fluids* **16**, 577.
HASOON, M. A. & MARTIN, B. W. 1977 *Proc. Roy. Soc.* A **352**, 351.
HUGHES, T. H. & REID, W. H. 1968 *Phil. Trans. Roy. Soc.* A **263**, 57.
KAYE, J. & ELGAR, E. C. 1958 *Trans. A.S.M.E.* **80**, 753.
KRUEGER, E. R. & DIPRIMA, R. C. 1964 *J. Fluid Mech.* **19**, 528.
SNYDER, H. A. 1962 *Proc. Roy. Soc.* A **265**, 198.
SNYDER, H. A. 1965 *Ann. Phys.* **31** (2), 292.
SPARROW, E. M., MUNRO, W. D. & JONSSON, V. K. 1964 *J. Fluid Mech.* **20**, 35.
TAYLOR, G. I. 1923 *Phil. Trans. Roy. Soc.* A **223**, 289.
THOMAS, A. D. 1974 Ph.D. thesis, University of Western Australia.